Biotechnol Lett (2015) 37:2497–2506
DOI 10.1007/s10529-015-1939-5

ORIGINAL RESEARCH PAPER

In vivo repair of rat transected sciatic nerve by low-intensity pulsed ultrasound and induced pluripotent stem cells-derived neural crest stem cells

Yonggang Lv · Panpan Nan · Guobao Chen · Yongqiang Sha · Bin Xia · Li Yang

Received: 14 July 2015 / Accepted: 13 August 2015 / Published online: 25 August 2015

Abstract
Objectives To evaluate the effects of the combination of low-intensity pulsed ultrasound (LIPUS) and induced pluripotent stem cells-derived neural crest stem cells (iPSCs-NCSCs) on the regeneration of rat transected sciatic nerve in vivo.
Results Tissue-engineered tubular nerve conduit was fabricated by electrospinning aligned nanofibers in longitudinal direction. This sustained the iPSCs-NCSCs and could be used as a bridge in rat transected sciatic nerve. Treatment with 0.3 W cm^{-2} LIPUS for 2 weeks and 5 min per day significantly improved the sciatic functional index, static sciatic function index and nerve conduction velocity of rat sciatic nerve. Histological analysis showed that there were more regenerative new blood vessels and new neurofilaments, higher expression level of β-III tubulin (Tuj1) in the experimental group seeded with iPSCs-NCSCs and stimulated with LIPUS.
Conclusion Combination of LIPUS with iPSCs-NCSCs promoted the regeneration and reconstruction of rat transected sciatic nerve and is an efficient and cost-effective method for peripheral nerve regeneration.

Keywords Induced pluripotent stem cells · Low-intensity pulsed ultrasound · Nerve regeneration · Sciatic nerve repair

Electronic supplementary material The online version of this article (doi:10.1007/s10529-015-1939-5) contains supplementary material, which is available to authorized users.

Y. Lv · P. Nan · G. Chen · Y. Sha · B. Xia · L. Yang
Key Laboratory of Biorheological Science and Technology (Chongqing University), Ministry of Education, Bioengineering College, Chongqing University, Chongqing 400044, People's Republic of China
e-mail: 939378180@qq.com

G. Chen
e-mail: chenguobao1985@163.com

Y. Sha
e-mail: shaziwait@126.com

B. Xia
e-mail: xiabin321@163.com

L. Yang
e-mail: yanglibme@cqu.edu.cn

Y. Lv · P. Nan · G. Chen · Y. Sha · B. Xia · L. Yang
'111' Project Laboratory of Biomechanics and Tissue Repair, Bioengineering College, Chongqing University, Chongqing 400044, People's Republic of China

Y. Lv (✉)
Mechanobiology and Regenerative Medicine Laboratory, Bioengineering College, Chongqing University, 174 Shazheng Jie, Shapingba, Chongqing 400044, People's Republic of China
e-mail: yglv@cqu.edu.cn

Introduction

Peripheral nerve injury is large-scale problem affecting more than one million people worldwide annually (Sun et al. 2009). Autografting technique is, by far, the most common method to compensate for peripheral nerve injuries and still is the gold standard for bridging nerve gaps. However, this approach has some serious drawbacks such as number and length of available donor nerve, the second surgery associated with donor site morbidity, insufficient functional outcome, aberrant regeneration etc. Alternative approaches to repair injured peripheral nerve are thus required. Various forms of external physical stimulation (electric stimulation, laser stimulation, ultrasound, magnetic field, and so on) can enhance the functional recovery of injured peripheral nerve (Mendonça et al. 2003; Shen et al. 2013; Kim et al. 2013; Beck-Broichsitter et al. 2014). Mendonça et al. (2003) found that low intensity, directly applied electric stimulation (1 μA) enhanced both morphologic and functional regeneration of rat crushed sciatic nerve. Low-level laser stimulation is another efficient technique in peripheral nerve recovery. Shen et al. (2013) applied low-level laser stimulation (660 nm) on the nerve conduit-implant site in a 15 mm transected sciatic nerve of rat for 2 weeks. Their results showed that low-level laser stimulation could improve motor function, enhance electrophysiological reaction, reduce muscle atrophy, and promote histomorphometric recovery. In addition, pulsed magnetic field therapy also has a positive influence on the functional regeneration of rat after a median nerve injury (Beck-Broichsitter et al. 2014).

As a type of safe and non-invasive physical stimulation factor, low-intensity ultrasound can promote tissue regeneration by improving of blood circulation, acceleration of wound healing and stimulation of angiogenesis (Kim et al. 2013). Lee et al. (2014) utilized low-intensity ultrasound to induce the differentiation of neural stem/progenitor cells (NSPCs) into neural cells and to improve neurite outgrowth. They showed that low-intensity ultrasound was a potential candidate for NSPCs induction and neural cell therapy. Tsuang et al. (2011) revealed that the intervention of low-intensity pulsed ultrasound (LIPUS) could promote primary cultured Schwann cells proliferation and prevent cell death, especially in a severely injured condition. In our previous research, the effect of LIPUS on the induced pluripotent stem cell-derived neural crest stem cells (iPSCs-NCSCs) was tested in vitro and the results showed that LIPUS had a positive effect on the viability, proliferation and neural differentiation of iPSCs-NCSCs (Lv et al. 2013). The efficient and cost-effective method of LIPUS acting on iPSCs-NCSCs expanded their use on neural differentiation in vivo. The present in vivo study further investigated the repair efficiency of the combination of LIPUS and iPSCs-NCSCs in rat transected sciatic nerve.

Materials and methods

Characterization of nanofibrous scaffold

Electrospinning technique was used to construct poly(L-lactic acid) (PLLA) nanofiber scaffold using a similar setup described previously study (Li et al. 2011). The detail is given in Supporting Information. The morphology of nanofibrous scaffold was characterized by filed emission scanning electron microscope (FESEM) with an accelerating voltage of 10 kV after coated with gold. Randomly selecting about 100 fibers from the FESEM images, the diam. of the nanofibers was measured by image analysis software (Image-Pro Plus, USA). Degree of alignment was calculated by measuring the orientation angles of the nanofibers with respect to the direction of the rotating collector.

Fabrication of PLLA nerve conduit

Nanofibrous scaffold was prepared at 33 mm × 15 mm (length × width) and rolled on a cylindrical stainless steel stent (outer diam. = 1 mm) which was covered with a water-soluble film. When the thickness of the nerve conduit reached 0.2 mm, the stent was immersed into deionized water after fixation. After the water-soluble film totally dissolved, nanofibrous nerve conduit (inner diam. = 1 mm and outer diam. = 1.2 mm) was obtained. All nerve conduits were sterilized with 75 % ethyl alcohol before in vivo implantation studies.

Mechanical testing

Mechanical properties of nerve conduit were measured by using a tabletop uniaxial testing instrument

(Instron-E1000, USA) under a cross-head speed of 10 mm min^{-1} at ambient condition. All samples were prepared in cylindrical shape at 40 mm × 1 mm × 1.2 mm (length × inner diam. × outer diam.) from the electrospun nanofibrous scaffold. Three samples were measured and each one was repeated three times.

Preparation of iPSCs-NCSCs seeded conduit

The iPSCs-NCSCs used in this study were from Prof. Li Song at University of California, Berkeley. iPSCs-NCSCs were cultured as described previously (Supporting Information) (Wang et al. 2011; Lv et al. 2013). Nerve conduits were sterilized with 75 % (v/v) ethyl alcohol before use. iPSCs-NCSCs suspended in SFM (10^4 cells μl^{-1}) were mixed with cold Matrigel solution (Sigma, USA) at 2:1 (v/v), and then were injected into the nanofibrous nerve conduit (e.g., 40 µl for one conduit). Consequently, the total number of iPSCs-NCSCs in each conduit was approx. 4×10^5. After each end of the tissue-engineered conduits had been tied, the conduits were covered by iPSCs-NCSCs maintenance medium and then held at 37 °C for 1 h. The conduits were further cultured for 24 h after the ends were untied. A 4–5 mm partial conduit was then cut in the middle portion of the nerve conduit. The conduit was dissected in lognitudinal section and live/dead assay was used to detect the viability of iPSCs-NCSCs in the tissue-engineered nerve conduit.

Animal experimental design and surgery

Twenty adult female Sprague–Dawley (SD) rats, 200–250 g, were used. The Institutional Animal Care and Use Committee approved all of the animal experimental protocols. Five experimental groups were set: (1) autograft group (represented as Autograft) (n = 4), (2) PLLA conduit group (represented as C) (n = 4), (3) PLLA conduit stimulated with LIPUS group (represented as C/LIPUS) (n = 4), (4) PLLA conduit seeded with iPSCs-NCSCs group (represented as C/iPSCs) (n = 4), and (5) PLLA conduit seeded with iPSCs-NCSCs and stimulated with LIPUS group (represented as C/iPSCs/LIPUS) (n = 4).

Animals were anaesthetized by intraperitoneal injection of 7 % (v/v) chloral hydrate (0.5 ml per 100 g). After the rat hair was scraped off, operation was taken with a scalpel under a 10 × surgical microscope in aseptic condition. Six mm nerve trunk was cut off and then a nerve conduit/autograft of 12 mm length was inserted between the two nerve stumps. One mm of each nerve end was inserted into the conduit. Thus, a gap of 10 mm was formed between the two stumps. The suture of graft was carried out under the surgical microscope with 9-0 suture, and the sutures of muscles and skin incision were conducted with 4-0 suture. Post-operatively, the SD rats were placed under a warm light for recovering from anesthesia and then housed separately with a free access to food and water in cage at 19–22 °C and a humidity of 40–50 % in a 12:12 light–dark cycle (Wang et al. 2011).

Low-intensity pulsed ultrasound (LIPUS) treatment

24 h after surgery, the LIPUS apparatus (US10, Cosmogamma, Italy) was employed to the incision site of the rat through a probe with 5 cm^2 working surface area. The parameters were set before each treatment: frequency, 1 MHz; pulse repetition rate (PRR), 100 Hz; duty cycle, 20 %; intensity, 0.3 W cm^{-2}; treatment time per day, 5 min; duration, 2 weeks. The probe was gently attached to the incision site. Coupling gel was coated between the ultrasonic transducer and the rat.

Gross observation

The wound healing, foot ulcer, atrophy of limp and muscle were observed after surgery. Dissection was carried out at 3 months after surgery. Gross observation of the connection between nerve conduit and sciatic nerve in the rats was conducted.

Nerve function analysis

Walking track analysis was carried out to test sciatic function of animal at 1 and 3 months. The plantar hind feet of animals were dyed with red ink for the test and trained to walk down a white sheet of paper with 60 cm long and 10 cm wide in a darkened enclosure. The sciatic functional index (SFI) and static sciatic function index (SSI) were obtained according to previous report (Supporting Information Amado et al. 2008).

Electrophysiology

Electrophysiological evaluation was made prior to graft harvesting with a multichannel intelligent physical record and analysis system (RM-6280, China) to assess the functional recovery of the sciatic nerve across the conduits directly. After anaesthesia with 7 % (w/v) chloral hydrate (0.5 ml per 100 g) via intraperitoneal injection, the sciatic nerve interposed with conduit was carefully re-exposed and dissected from surrounding tissue. A bipolar hook stimulating electrode was placed at the proximal end of the nerve, and two recording electrodes were placed at the medium and distal positions of sciatic nerve, respectively. A ground electrode was placed in a superficial muscle layer around the skin. The distance between every two electrodes was measured with a vernier caliper. Stimuli (3 V) was delivered to the sciatic nerve for 0.2 ms from a stimulator of the RM-6280 data acquisition system. The response was stored on a computer and data was captured. The latencies were measured from the stimulating electrode to recording electrode. Nerve conduction velocity (NCV) was calculated through dividing the distance between two recording electrodes by the average latency difference between the compound action potential (CAP) at these two recording electrodes. Electrical stimulation was repeated 10 times and averaged per rat to determine the NCV.

Histological analysis

Histological analysis was carried out after electrophysiology testing. The nerve conduits were harvested immediately and fixed in 4 % (v/v) paraformaldehyde at 4 °C for 24 h followed by 30 % (w/v) sucrose at 3 months post-implantation. 2 mm graft in the middle portion (5–7 mm from the proximal end of the graft) in each group was embedded into optimum cutting temperature (OCT). Cross Sects. (10 μm thickness) were cut in freezing microtome for hematoxylin/eosin (HE) staining, Bielschowsky staining and immunostaining using the mouse monoclonal antibodies against β-III tubulin (Tuj1; 1:1000), rabbit polyclonal antibodies against neurofilament (NFM) (1:200), rabbit polyclonal antibodies against S100β (1:500) and mouse monoclonal antibodies against GFAP (1:500;).

Statistical analysis

All results were presented as mean ± standard deviation (SD). Comparisons among groups were performed by One-way analysis of ANOVA. A statistical significance was represented as $*P < 0.05$ and an extremely statistical significance was represented as $**P < 0.01$, respectively.

Results

Characterization of nanofibrous scaffold

Field emission scanning electron microscopy (FESEM) images showed that the PLLA nanofibers arranged in parallel in one direction and had good alignment (Supplementary Fig. 1a). The diam. of individual nanofiber ranged from 100–400 nm and the mean diam. was 251.7 ± 59.4 nm (Supplementary Fig. 1b). More than 75 % of the nanofibers lay within 10 degree to the direction of rotating axis (Supplementary Fig. 1c).

Construction of tissue engineered conduit

Figure 1a outlines the tissue engineering approach to fabricate the tissue engineered nerve conduit. The PLLA nerve conduit was a hollow tube with aligned nanofibers in longitudinal direction, which could promote axon growth (Wang et al. 2011). The length of fabricated conduit was 15 mm (Fig. 1b). When the conduit was grafted in vivo, it could be managed up to 12 mm to be inserted into the nerve defect. It has an inner diam. of ~1 mm and outer diam. of about 1.2 mm (Fig. 1c). Figure 1d describes the typical tensile stress–strain curve of the nerve conduit. Young's modulus and tensile strength of PLLA conduit were 34.49 ± 0.47 MPa and 1.86 ± 0.21 MPa, respectively. The cell viability in the conduit was evaluated by live/dead assay, which showed that >95 % of iPSCs-NCSCs survived in the PLLA nerve conduit after culture in vitro for 1 day (Fig. 2). These tissue engineered conduits were kept in a cell culture incubator for 1 day prior to surgery.

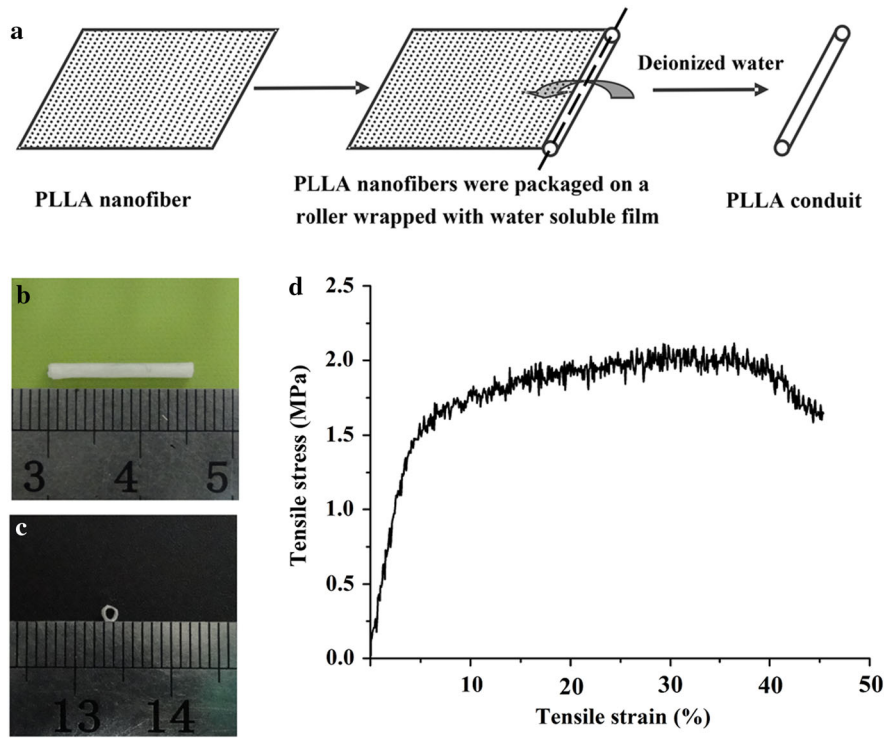

Fig. 1 PLLA nanofibrous nerve conduit for sciatic nerve regeneration. **a** Schematic outline of fabrication process of PLLA nerve conduit. **b** The length of PLLA nerve conduit was 15 mm. **c** The inner diam. and outer diam. of PLLA nerve conduit were 1 and 1.2 mm. **d** The representative tensile stress–strain curve of PLLA conduit. Young's modulus and tensile strength of PLLA conduit were 34.49 ± 0.47 and 1.86 ± 0.21 MPa, respectively

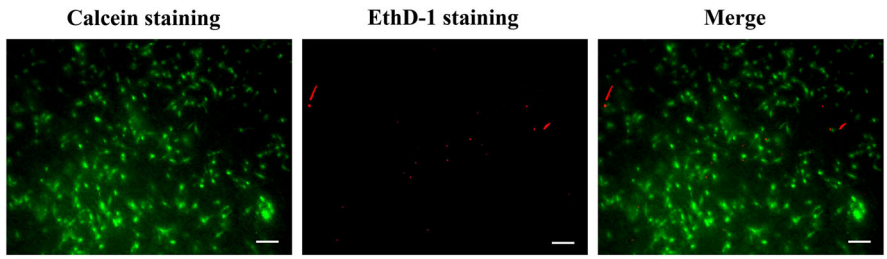

Fig. 2 Live/dead staining of live and dead iPSCs-NCSCs in the longitudinal section of nerve conduit. The iPSCs-NCSCs mixed with Matrigel were injected in the PLLA nerve conduit and cultured for 24 h in vitro. The viability of the iPSCs-NCSCs in the tissue engineered nanofibrous nerve conduit was conducted through live/dead assay. Live cells were labeled with *green* fluorescence by calcein and dead cells were labeled with *red* fluorescence by EthD-1. *Scale bar* 200 μm

Post-operative gross observation

The wound healing, foot ulcers, the atrophy of limp and muscle were observed after operative procedure. Swelling was occasionally found in the SD rats at 24 h post-operation and gradually disappeared after 3 days. Muscle atrophy could be found in some rats at 1 month post-operation. But, all of them could be alleviated at 3 months. There was slight inflammation in group C and group C/iPSCs and no obvious inflammation reaction was observed in other groups. Connective tissue wrapped on the graft was observed in all groups. There was no neuroma formation at the interface between nerve conduit and sciatic nerve after anatomy in all animals at 3 months postsurgery (Supplementary Fig. 2).

Footprint analysis

Figure 3 shows the values of SFI and SSI at 1 and 3 months post-implantation. With or without seeding iPSCs-NCSCs, low-intensity pulsed ultrasound

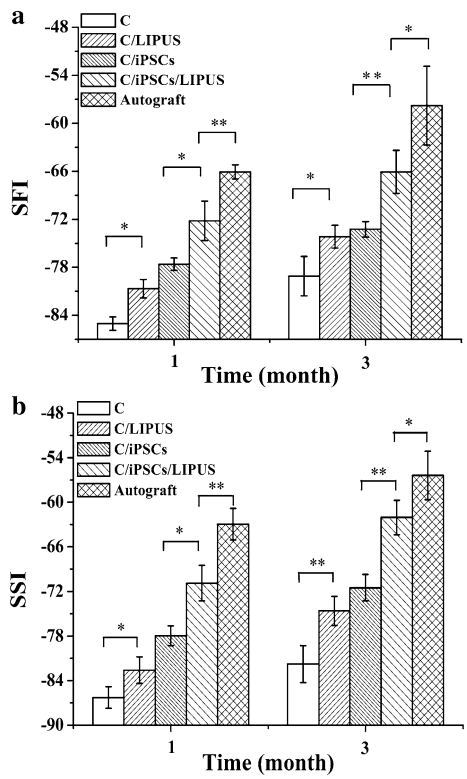

Fig. 3 Mean values for the SFI (**a**) and SSI (**b**) at 1 and 3 months post-operation. C, C/LIPUS, C/iPSCs, C/iPSCs/LIPUS and Autograft represent PLLA conduit group, PLLA conduit stimulated with LIPUS group, PLLA conduit seeded with iPSCs-NCSCs group, PLLA conduit seeded with iPSCs-NCSCs and stimulated with LIPUS group, and autograft group. Data was presented as mean ± SD (*$P < 0.05$, **$P < 0.01$)

(LIPUS) significantly improved the SFI and SSI values at 1 and 3 months post-implantation. The SFI and SSI values in group C/LIPUS exceeded those in group C while the SFI and SSI values in group C/iPSCs/LIPUS were larger than those in group C/iPSCs ($P < 0.05$). In all experimental groups, both SFI and SSI substantially increased over time. In group Autograft, SFI and SSI were increased from -66.08 ± 0.89 at 1 month to -57.79 ± 4.93 at 3 months ($n = 4$, $P < 0.05$), and from -62.96 ± 2.12 at 1 month to -56.39 ± 3.28 at 3 months ($n = 4$, $P < 0.05$), respectively. The SFI and SSI in group Autograft were significantly larger than those in other groups ($P < 0.05$), which implied that animals in group Autograft have the fastest nerve recovery than animals in other groups.

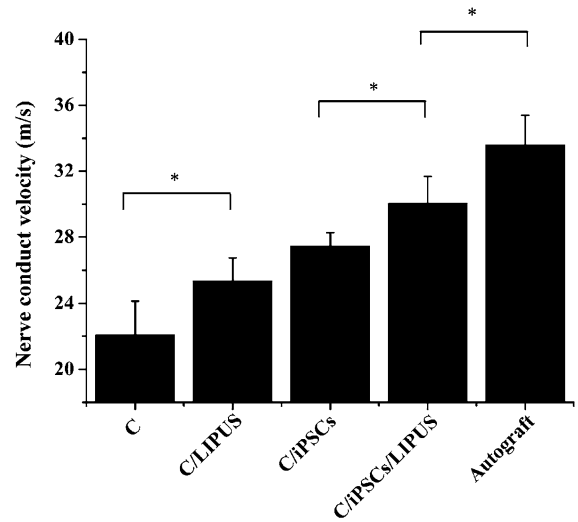

Fig. 4 Nerve conduction velocities at 3 months post-implantation in PLLA conduit group (C), PLLA conduit stimulated with LIPUS group (C/LIPUS), PLLA conduit seeded with iPSCs-NCSCs group (C/iPSCs), PLLA conduit seeded with iPSCs-NCSCs and stimulated with LIPUS group (C/iPSCs/LIPUS) and autograft group (Autograft). Data was presented as mean ± SD (*$P < 0.05$)

Electrophysiologic assessment

Figure 4 shows the NCV at 3 months post-implantation. Without seeding iPSCs-NCSCs, LIPUS significantly improved the NCV from 22.07 ± 2.06 m s^{-1} (C) to 25.34 ± 1.41 m s^{-1} (C/LIPUS) ($n = 4$, $P < 0.05$). After seeded iPSCs-NCSCs, NCV was increased from 27.45 ± 0.82 m s^{-1} (C/iPSCs) to 30.03 ± 1.66 m s^{-1} (C/iPSCs/LIPUS) by LIPUS ($n = 4$, $P < 0.05$). However, the NCV in group Autograft (33.58 ± 1.81 m s^{-1}) was still significantly higher than those in other four groups ($n = 4$, $P < 0.05$).

Histological evaluation

HE staining analysis was performed to evaluate the regenerated nerves in different groups (Fig. 5). In group C, there are few cells in the lumen of the conduit. The cell distribution locations between group C/LIPUS and group C/iPSCs are different. The cells located close to the conduit surface in group C/LIPUS due to the function of LIPUS while the cells stayed in the lumen of conduit in group C/iPSCs. Compared with other groups,

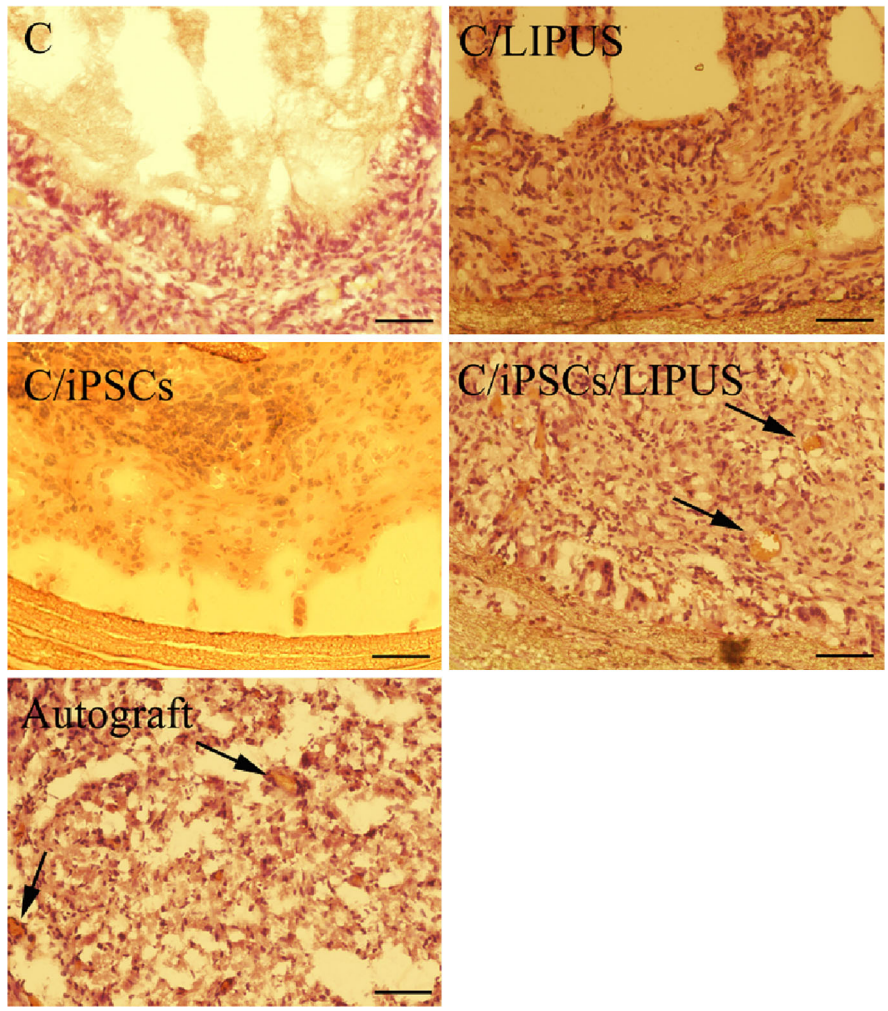

Fig. 5 HE staining of sciatic nerve in the cross section of nerve conduit at 5–7 mm from the proximal end at 3 months post-implantation. C, C/LIPUS, C/iPSCs, C/iPSCs/LIPUS and Autograft represent PLLA conduit group, PLLA conduit stimulated with LIPUS group, PLLA conduit seeded with iPSCs-NCSCs group, PLLA conduit seeded with iPSCs-NCSCs and stimulated with LIPUS group, and autograft group. *Arrow* indicates typical blood vessel. *Scale bar* 100 μm

there were more new neurofilaments and new blood vessels in group C/iPSCs/LIPUS and group Autograft.

After Belschowsky staining the regenerated nerve axon is black and the nucleus a light brown. In group Autograft, the new neuofilaments had a large density and arranged closely. In group C/LIPUS and group C/iPSCs/LIPUS, regenerated neuofilaments were clearly visible with neat arrangement and uniform distribution. However, group C/iPSCs only had a small quantity of regenerated nerve axons in the lumen center of conduit (data not shown). There were fewer regenerative nerve fibers with the scattered axons distribution in group C and group C/iPSCs compared with group C/LIPUS and group C/iPSCs/LIPUS (Fig. 6).

Tuj1 is the early neural differentiation marker. Immunofluorescence staining for Tuj1 showed that there were much larger numbers neurons in group Autograft, group C/iPSCs/LIPUS and group C/iPSCs than group C and group C/LIPUS (Fig. 7). In addition, the positive staining of Tuj1 in group C/iPSCs/LIPUS is higher than those in group C/LIPUS and group C/iPSCs. As one of the three major neurofilaments (NF) subunits, NFM represents the main cytoskeletal elements in mature neuron. However, NFM has not been expressed obviously in our experiments (data not shown). Schwann cells-specific proteins including S100β and GFAP could either not been detected (data not shown).

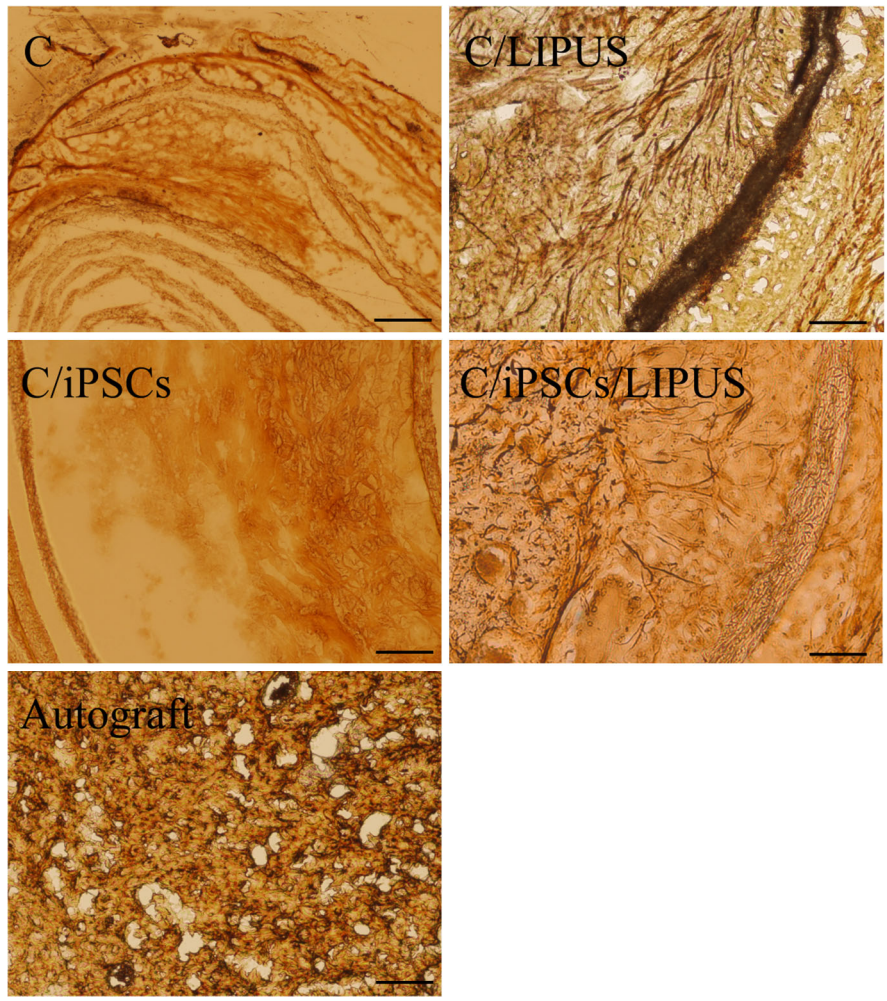

Fig. 6 Bielschowsky staining of sciatic nerve in the cross section of nerve conduit at 5–7 mm from the proximal end at 3 months post-implantation. C, C/LIPUS, C/iPSCs, C/iPSCs/LIPUS and Autograft represent PLLA conduit group, PLLA conduit stimulated with LIPUS group, PLLA conduit seeded with iPSCs-NCSCs group, PLLA conduit seeded with iPSCs-NCSCs and stimulated with LIPUS group, and autograft group. The regenerated nerve axons were *black* and the nucleus were *light brown* with pale *yellow* background. *Scale bar* 100 μm

Discussion

Using low-intensity pulsed ultrasound (LIPUS) to repair damaged peripheral nerve has been investigated in many studies. However, the optimal therapeutic intensity of LIPUS acted on the nerve conduit in vivo is still unclear. Our previously study (Lv et al. 2013) proved that LIPUS at 0.3 and 0.5 W cm^{-2} could enhance the viability and proliferation of iPSCs-NCSCs. Tsuang et al. (2011) also demonstrated that 0.3 W cm^{-2} LIPUS could promote Schwann cells proliferation and prevent cell death in a severely injured peripheral nerve. Therefore, the intensity of LIPUS selected in this study was 0.3 W cm^{-2}. Gross observation of the sciatic nerve at 3 months post-operation showed no obvious inflammation in group Autograft and the other two groups treated with LIPUS. One possible reason is that the mechanical function of LIPUS enhanced blood and lymph circulation in the lesions and sped up cleaning the deforming tissue by enhancing the activity of macrophages to reduce inflammation (Chen et al. 2010). Another possible reason is that LIPUS has the anti-inflammatory effect with reduced infiltration of inflammatory cells in the defect area (Chung et al. 2012).

SFI and SSI are simple and repeatable measures to evaluate the recovery condition of sciatic nerve injury from the normal and experimental footprints. Compared with the groups with sham LIPUS treatment, experimental groups treated with LIPUS have better functional recovery at one and 3 months. Especially at 3 months, the difference was extremely significant between group C/iPSCs/LIPUS and other three

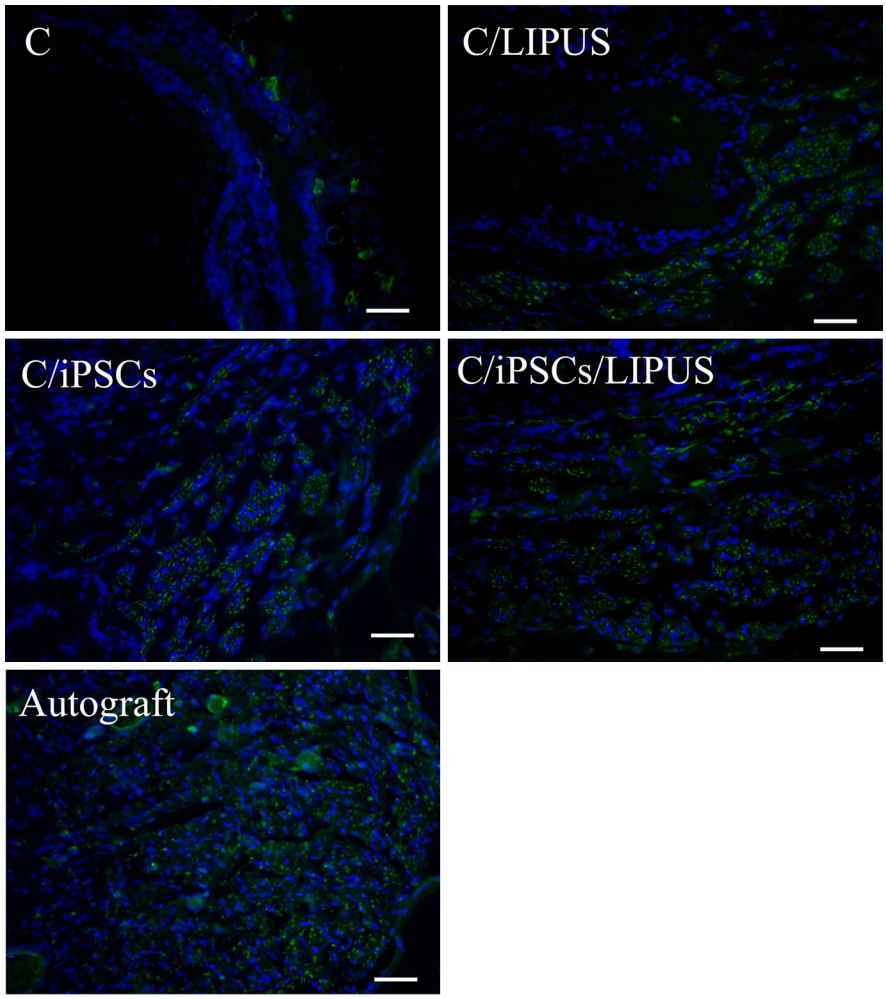

Fig. 7 Immunostaining of Tuj1 of sciatic nerve in the cross section of nerve conduit at 5–7 mm from the proximal end at 3 months post-implantation. C, C/LIPUS, C/iPSCs, C/iPSCs/LIPUS and Autograft represent PLLA conduit group, PLLA conduit stimulated with LIPUS group, PLLA conduit seeded with iPSCs-NCSCs group, PLLA conduit seeded with iPSCs-NCSCs and stimulated with LIPUS group, and autograft group. *Arrow* indicates typical blood vessel. *Scale bar* 50 μm

experiment groups (group C, group C/iPSCs and group C/LIPUS). These findings suggested that LIPUS can improve walking ability in nerve injured rat in a certain period of time. The results of electrophysiological tests confirmed the results of SFI and SSI. At the same time point after surgery, NCV in the groups with LIPUS stimulation were higher than that in the groups with sham LIPUS treatment regardless of iPSCs-NCSCs-seeded. This finding demonstrated that combination of LIPUS and iPSCs has a positive effect on the repair of injured nerve.

The results of HE staining, Bielschowsky staining and immunofluorescent staining of Tuj1 showed that nerve filaments in groups treated by LIPUS had a greater density. There were also numbers of blood vessels in group C/iPSCs/LIPUS and group Autograft. The outcome may be caused by the application of iPSCs-NCSCs and LIPUS in this study. On one hand, iPSCs-NCSCs can differentiate into vascular cells and neurons, which could accelerate the vascular and nerve regeneration during the restore of injured nerve (Kane et al. 2011). On the other hand, LIPUS could induce angiogenesis (Hanawa et al. 2014) and promote neural differentiation (Lv et al. 2013). In addition, LIPUS could speed up the exchanges of nutrients and toxic substances which are good for the formation of nerve filaments (Chen et al. 2010). The result of Tuj1 immunofluorescence staining suggested that LIPUS and iPSCs-NCSCs can promote the neuron regeneration. The regenerated neurons also could secrete some growth factors such as neural growth factor (NGF) and brained-derived neural growth factor (BDNF), which were benefit for the reconstruction of synapses. In our previously study (Lv et al. 2013), the gene and protein

expression levels of Schwann cells-specific markers (S100β and GFAP) were enhanced by LIPUS treatment in vitro. The present findings supported the hypothesis that the combination of LIPUS with iPSCs-NCSCs had a positive effect on the nerve regeneration after peripheral nerve injury in vivo.

In conclusion, our study suggested that LIPUS can promote peripheral nerve regeneration by using a tissue-engineered nerve conduit seeded with iPSCs-NCSCs. In vivo evaluation in rat showed that the sciatic function and the NCV were both accelerated when conduit was seeded with iPSCs-NCSCs and treated by LIPUS. It is also revealed that the combination LIPUS with iPSCs-NCSCs could promote angiogenesis and regeneration of nerve fiber and neuron differentiation. This study contributes to the development of safe and effective therapeutic strategies for the regeneration of peripheral nerve injury.

Acknowledgments This work was supported in part by grants from the National Natural Science Foundation of China (11172338), the Fundamental Research Funds for the Central Universities (CQDXWL-2012-Z001), and the Sharing Fund of Chongqing University's Large-scale Equipment.

Supporting information Supplementary experimental methods (Cell culture; Preparation of electrospun solution and electrospinning; Nerve function analysis).

Supplementary Fig. 1—Characteristic of PLLA nanofibers.

Supplementary Fig. 2—Gross observation of the nerve conduits.

Compliance with ethical standards

Conflict of interest The authors declare that they have no conflict of interests.

References

Amado S, Simões MJ, Armada da Silva PA, Luís AL, Shirosaki Y, Lopes MA, Santos JD, Fregnan F, Gambarotta G, Raimondo S, Fornaro M, Veloso AP, Varejão AS, Maurício AC, Geuna S (2008) Use of hybrid chitosan membranes and N1E–115 cells for promoting nerve regeneration in an axonotmesis rat model. Biomaterials 29:4409–4419

Beck-Broichsitter BE, Lamia A, Geuna S, Fregnan F, Smeets R, Becker ST, Sinis N (2014) Does pulsed magnetic field therapy influence nerve regeneration in the median nerve model of the rat? Biomed Res Int 2014:401760

Chen WZ, Qiao H, Zhou W, Wu JR, Wang ZB (2010) Upgraded nerve growth factor expression induced by low-intensity continuous-wave ultrasound accelerates regeneration of neurotometicly injured sciatic nerve in rats. Ultrasound Med Biol 36:1109–1117

Chung JI, Barua S, Choi BH, Min BH, Han HC, Baik EJ (2012) Anti-inflammatory effect of low intensity ultrasound (LIUS) on complete Freund's adjuvant-induced arthritis synovium. Osteoarthritis Cartilage 20:314–322

Hanawa K, Ito K, Aizawa K, Shindo T, Nishimiya K, Hasebe Y, Tuburaya R, Hasegawa H, Yasuda S, Kanai H, Shimokawa H (2014) Low-intensity pulsed ultrasound induces angiogenesis and ameliorates left ventricular dysfunction in a porcine model of chronic myocardial ischemia. PLoS One 9:e104863

Kane NM, Xiao Q, Baker AH, Luo Z, Xu Q, Emanueli C (2011) Pluripotent stem cell differentiation into vascular cells: a novel technology with promises for vascular regeneration. Pharmacol Ther 129:29–49

Kim JR, Oh SH, Kwon GB, Namgung U, Song KS, Jeon BH, Lee JH (2013) Acceleration of peripheral nerve regeneration through asymmetrically porous nerve guide conduit applied with biological/physical stimulation. Tissue Eng Part A 19:2674–2685

Lee IC, Lo TL, Young TH, Li YC, Chen NG, Chen CH, Chang YC (2014) Differentiation of neural stem/progenitor cells using low-intensity ultrasound. Ultrasound Med Biol 40:2195–2206

Li L, Li H, Qian Y, Li X, Singh GK, Zhong L, Liu W, Lv Y, Cai K, Yang L (2011) Electrospun poly(ε-caprolactone)/silk fibroin core-sheath nanofibers and their potential applications in tissue engineering and drug release. Int J Biol Macromol 49:223–232

Lv Y, Zhao P, Chen G, Sha Y, Yang L (2013) Effects of low-intensity pulsed ultrasound on cell viability, proliferation and neural differentiation of induced pluripotent stem cells-derived neural crest stem cells. Biotechnol Lett 35:2201–2212

Mendonça AC, Barbieri CH, Mazzer N (2003) Directly applied low intensity direct electric current enhances peripheral nerve regeneration in rats. J Neurosci Methods 129: 183–190

Shen CC, Yang YC, Huang TB, Chan SC, Liu BS (2013) Neural regeneration in a novel nerve conduit across a large gap of the transected sciatic nerve in rats with low-level laser phototherapy. J Biomed Mater Res A 101:2763–2777

Sun W, Sun C, Zhao H, Lin H, Han Q, Wang J, Ma H, Chen B, Xiao Z, Dai J (2009) Improvement of sciatic nerve regeneration using laminin-binding human NGF-beta. PLoS One 4:e6180

Tsuang YH, Liao LW, Chao YH, Sun JS, Cheng CK, Chen MH, Weng PW (2011) Effects of low intensity pulsed ultrasound on rat Schwann cells metabolism. Artif Organs 35:373–383

Wang A, Tang Z, Park IH, Zhu Y, Patel S, Daley GQ, Li S (2011) Induced pluripotent stem cells for neural tissue engineering. Biomaterials 32:5023–5032